Alleviation of catastrophic quenching in solar dynamo model with nonlocal alpha-effect

L.L. Kitchatinov[1,2,⋆] and **S.V. Olemskoy**[1]

[1] Institute for Solar-Terrestrial Physics, P.O. Box 291, Irkutsk 664033, Russia
[2] Pulkovo Astronomical Observatory, St. Petersburg 196140, Russia

The dates of receipt and acceptance should be inserted later

Key words Sun: magnetic fields – stars: magnetic fields – magnetohydrodynamics (MHD) – turbulence

The nonlocal alpha-effect of Babcock-Leighton type is not prone to the catastrophic quenching due to conservation of magnetic helicity. This is shown with a dynamo model, which jointly applies the nonlocal alpha-effect, the diamagnetic pumping, and dynamical equation for the magnetic alpha-effect. The same model shows catastrophic quenching when the alpha-effect is changed to its local formulation. The nonlocal model shows the preferred excitation of magnetic fields of dipolar symmetry, which oscillate with a period of about ten years and have a toroidal-to-polar fields ratio of about a thousand.

1 Introduction

This paper suggest a solution for the problem of so-called 'catastrophic quenching' of the alpha-effect of the mean-field dynamo theory. The standard alpha-effect of helical turbulent motions (Parker 1955; Steenbeck, Krause & Rädler 1966) with its standard (algebraic) quenching by a magnetic field (Moffatt 1972; Rüdiger 1974; Roberts & Soward 1975; Rüdiger & Kitchatinov 1993) is only a part of the total alpha-effect known in the mean-field theory. Friesh et al. (1975) were probably the first to notice that not only helical motions but small-scale helical magnetic fields produce the alpha-effect. This magnetic contribution was later recognised to lead to the catastrophic quenching of the total alpha-effect (Vainshtein & Cattaneo 1992; Gruzinov & Diamond 1994; Blackman & Brandenburg 2002).

The term 'catastrophic' is used in the sense that the argument of the quenching function is $\mathrm{R_m}B^2/B_{\rm eq}^2$, not just $B^2/B_{\rm eq}^2$ as in the case of a standard algebraic quenching ($\mathrm{R_m}=\eta_{\rm t}/\eta$ is the ratio of turbulent $\eta_{\rm t}$ to microscopic η magnetic diffusivity, and $B_{\rm eq}=\sqrt{\mu\rho}\,u'_{\rm rms}$ is the energy equipartition value of a magnetic field). The magnetic Reynolds number, $\mathrm{R_m}$, in astrophysical fluids is normally so large that even a very small mean field B suppresses the alpha-effect in the case of catastrophic quenching.

This type of magnetic quenching is related to the conservation of magnetic helicity. Its origin is, briefly, as follows. The large-scale magnetic fields generated by the alpha-effect dynamos are helical. As the magnetic helicity is conserved, small-scale magnetic fields attain helicity equal in amount and opposite in sign to that of large-scale fields. Helical small-scale fields produce their own magnetic alpha-effect that counteracts the acting alpha-effect of whatever origin so that the total alpha-effect vanishes. Detailed discussions of catastrophic quenching can be found in literature (cf., e.g., Brandenburg & Subramanian 2005).

Catastrophic quenching presents a serious problem for the cosmic dynamo theory. The currently leading idea in resolving the problem for the sun is the evacuation of small-scale magnetic helicity from the solar interior by helicity fluxes (Vishniac & Cho 2001; Guerrero, Chatterjee & Brandenburg 2010) and then from the solar corona by coronal mass ejections (Brandenburg 2009). However, coronal ejections can evacuate only a minor part of magnetic helicity (Kliem, Rust & Seehafer 2010).

This paper suggests another solution related to nonlocal formulation of the alpha-effect. If the region where the toroidal field is concentrated is spatially separated from the region where the poloidal field is produced by the alpha-effect, the large-scale fields generated will not be helical, and the problem of catastrophic quenching does not arise. To show this, we use a numerical model of the $\alpha\Omega$-dynamo with a nonlocal alpha-effect of the Babcock-Leighton type (cf., e.g., Dikpati & Charbonneau 1999). Another important ingredient of our model is the diamagnetic pumping of large-scale fields. The pumping ensures that toroidal fields are concentrated near the base of the convection zone away from the near-top region where the alpha-effect is active. The dynamical equation for the magnetic part of the alpha-effect is involved. This normally leads to a strong (catastrophic) suppression of the dynamo. We actually find catastrophic quenching when changing to a local formulation of the alpha-effect in our model. The nonlocal model, however, does not show any sign of catastrophic quenching. With the largest $\mathrm{R_m}=10^4$ we can apply, the results of the runs with the magnetic alpha-effect included or neglected are practically the same. The nonlocal model reproduces the main

⋆ Corresponding author: e-mail: kit@iszf.irk.ru

features of the solar cycle. There are also some disagreements with observations showing ways for model improvement.

2 The model

2.1 Dynamical equation for $\alpha_{\rm M}$

Our dynamo model is based on the mean-field induction equation

$$\frac{\partial \boldsymbol{B}}{\partial t} = \boldsymbol{\nabla}\times\left(\boldsymbol{\mathcal{E}} + \boldsymbol{u}\times\boldsymbol{B} - \eta\boldsymbol{\nabla}\times\boldsymbol{B}\right), \tag{1}$$

where η is the microscopic diffusivity, $\boldsymbol{u}$ is the mean velocity, and $\boldsymbol{E} = \langle \boldsymbol{u}'\times\boldsymbol{B}'\rangle$ is the mean electromotive force. The electromotive force in its local formulation,

$$\boldsymbol{\mathcal{E}} = \langle \boldsymbol{u}'\times\boldsymbol{B}'\rangle = (\alpha_{\rm K}+\alpha_{\rm M})\boldsymbol{B} + ..., \tag{2}$$

includes the magnetic alpha-effect $\alpha_{\rm M}$ together with the standard kinetic $\alpha_{\rm K}$.

The heuristic dynamical equation for the $\alpha_{\rm M}$

$$\frac{\partial \alpha_{\rm M}}{\partial t} + \boldsymbol{\nabla}\cdot\boldsymbol{\mathcal{F}} = -2\frac{\eta_{\rm t}}{\ell^2}\left(\frac{\boldsymbol{\mathcal{E}}\cdot\boldsymbol{B}}{B_{\rm eq}^2} + \frac{\alpha_{\rm M}}{\rm R_m}\right) \tag{3}$$

(Kleeorin & Ruzmaikin 1982; Blackman & Brandenburg 2002) can be formulated without specification of a particular form of the mean electromotive force $\boldsymbol{\mathcal{E}}$; ℓ is the correlation length. For a uniform mean field, however, Eq. (2) applies and the steady value of the total $\alpha = \alpha_{\rm K}+\alpha_{\rm M}$ can be estimated to be

$$\alpha = \frac{\alpha_{\rm K}}{1+{\rm R_m}\frac{B^2}{B_{\rm eq}^2}}. \tag{4}$$

This equation describes catastrophic quenching of the alpha-effect. We shall use the Eq. (3) in our model of solar dynamo to see that the dynamo is strongly suppressed when the local formulation (2) for the alpha-effect is applied. Note that the magnetic alpha-effect is local by nature in contrast to the kinetic alpha-effect that allows a nonlocal formulation (Blackman & Brandenburg 2002; Brandenburg & Käpylä 2007).

With a nonlocal formulation for the kinetic alpha-effect, the toroidal field may be small in the region where the alpha-effect is active. The $\alpha_{\rm M}$ is also small in this case and catastrophic quenching does not happen. We shall see that this possibility can indeed be realised in a dynamo model with a nonlocal (kinetic) alpha-effect.

2.2 Dynamo equations

Our model accounts for the diamagnetic pumping of mean fields with an effective velocity of

$$\boldsymbol{V}_{\rm dia} = -\frac{1}{2}\boldsymbol{\nabla}\eta_{\rm t}. \tag{5}$$

Diamagnetic pumping was predicted analytically by Zeldovich (1957) and Rädler (1968). The diamagnetic effect of inhomogeneous turbulence lacks pictorial explanation but its existence has been confirmed by direct numerical simulations (Brandenburg et al. 1996; Dorch & Nordlund 2001; Ziegler & Rüdiger 2003) and by laboratory experiment with turbulent liquid Sodium (Spence et al. 2007). The concentration of magnetic fields at the base of convection zone by the diamagnetic pumping can be important for a dynamo (Rüdiger & Brandenburg 1995; Guerrero & de Gouveia Dal Pino 2008; Kitchatinov & Rüdiger 2008).

With allowance for the diamagnetic pumping, the mean electromotive force reads

$$\boldsymbol{\mathcal{E}} = -\sqrt{\eta_{\rm T}}\,\boldsymbol{\nabla}\times\left(\sqrt{\eta_{\rm T}}\boldsymbol{B}\right) + \alpha_{\rm M}\boldsymbol{B} + \boldsymbol{\mathcal{A}}, \tag{6}$$

where $\eta_{\rm T} = \eta+\eta_{\rm t}$ is total magnetic diffusivity and $\boldsymbol{\mathcal{A}}$ stands for the contribution of the kinetic alpha-effect that can be written as

$$\boldsymbol{\mathcal{A}} = \int \hat{\alpha}(\boldsymbol{r},\boldsymbol{r}')\boldsymbol{B}(\boldsymbol{r}')\,{\rm d}^3r'. \tag{7}$$

With $\hat{\alpha} = \alpha_{\rm K}\delta(\boldsymbol{r}-\boldsymbol{r}')$, we recover the local alpha-effect. The kernel function $\hat{\alpha}$ for the nonlocal formulation will be specified later.

We will consider an axisymmetric dynamo in a spherical shell. The magnetic field in this case can be written as a superposition of its toroidal part B and a poloidal field defined with a toroidal potential A:

$$\boldsymbol{B} = \boldsymbol{e}_\phi B + \boldsymbol{\nabla}\times\left(\boldsymbol{e}_\phi\frac{A}{r\sin\theta}\right), \tag{8}$$

where standard spherical coordinates are used and $\boldsymbol{e}_\phi$ is the azimuthal unit vector.

Normalized variables are used. Time is measured in units of $R_\odot^2/\eta_0$; η_0 is the characteristic value of total diffusivity. The magnetic field is normalized to the field strength B_0 for which nonlinear effects become essential, and the α-parameter - to its characteristic value α_0. The poloidal field potential is measured in units of $\alpha_0 B_0 R_\odot^3/\eta_0$. From now on, the same notations are kept for the normalized variables as used before for their not normalized counterparts, except for the fractional radius $x = r/R_\odot$ and normalized diffusivity $\eta = \eta_{\rm T}/\eta_0$. The normalized equation for the toroidal field reads

$$\begin{aligned}\frac{\partial B}{\partial t} &= \frac{\mathcal{D}}{x}\left(\frac{\partial f}{\partial x}\frac{\partial A}{\partial\theta} - \frac{\partial f}{\partial\theta}\frac{\partial A}{\partial x}\right)\\ &+ \frac{\eta}{x^2}\frac{\partial}{\partial\theta}\left(\frac{1}{\sin\theta}\frac{\partial(\sin\theta B)}{\partial\theta}\right)\\ &+ \frac{1}{x}\frac{\partial}{\partial x}\left(\sqrt{\eta}\,\frac{\partial(\sqrt{\eta}\,xB)}{\partial x}\right),\end{aligned} \tag{9}$$

where

$$\mathcal{D} = \frac{\alpha_0\Omega R_\odot^3}{\eta_0^2} \tag{10}$$

is the dynamo number. The $\alpha\Omega$-approximation is applied to neglect the alpha-effect in the toroidal field equation (9). In this equation, f is the normalized rotation frequency,

$$\boldsymbol{u} = \boldsymbol{e}_\phi r\sin\theta\Omega f(x,\theta). \tag{11}$$

The equation for the poloidal field with nonlocal alpha-effect is written as

$$\frac{\partial A}{\partial t} = \frac{\eta}{x^2}\sin\theta\frac{\partial}{\partial\theta}\left(\frac{1}{\sin\theta}\frac{\partial A}{\partial\theta}\right) + \sqrt{\eta}\frac{\partial}{\partial x}\left(\sqrt{\eta}\frac{\partial A}{\partial x}\right) + x\sin\theta\cos\theta\int\limits_{x_{\rm i}}^{x}\hat{\alpha}(x,x')B(x',\theta)\,{\rm d}x' + \hat{\alpha}_{\rm M}B, \quad (12)$$

where $\hat{\alpha}_{\rm M} = x\sin\theta(\alpha_{\rm M}/\alpha_0)$ is the normalised magnetic alpha-parameter. The integration in this equation is only in the radius with the upper limit x. This qualitatively reflects the fact that the nonlocal alpha-effect in some point x is contributed by the buoyant magnetic loops rising from deeper layers ($x' < x$) of the convection zone and that buoyant velocities are almost vertical.

The equation system is closed with the dynamical equation for $\hat{\alpha}_{\rm M}$. We neglect the helicity flux in Eq. (3) and use the $\alpha\Omega$-approximation to rewrite this equation in normalized units:

$$\frac{\partial\hat{\alpha}_{\rm M}}{\partial t} = -2\hat{\eta}\left(\frac{R_\odot}{\ell}\right)^2\left(B\frac{\partial A}{\partial t} - \frac{\hat{\eta}}{x^2\sin\theta}\frac{\partial A}{\partial\theta}\frac{\partial(\sin\theta B)}{\partial\theta} - \frac{\sqrt{\hat{\eta}}}{x}\frac{\partial(\sqrt{\hat{\eta}}xB)}{\partial x}\frac{\partial A}{\partial x}\right) - 2\left(\frac{R_\odot}{\ell}\right)^2\frac{\hat{\alpha}_{\rm M}}{{\rm R_m}}, \quad (13)$$

where $\hat{\eta} = \eta_{\rm t}/\eta_0 = \eta - {\rm R_m^{-1}}$ is the normalized turbulent diffusivity. The magnetic alpha-effect and related catastrophic quenching can be switched off by omitting the last term in Eq. (12). Later on, we will compare the results obtained with account for the magnetic alpha effect and without it.

The boundary conditions assume an interface with a superconductor on the inner boundary of radius $x_{\rm i}$,

$$\frac{\partial\left(\sqrt{\eta}xB\right)}{\partial x} = 0, \quad A = 0 \quad \text{for} \quad x = x_{\rm i}, \quad (14)$$

and pseudo-vacuum conditions on the top,

$$B = 0, \quad \frac{\partial A}{\partial x} = 0 \quad \text{for} \quad x = 1. \quad (15)$$

2.3 Model design

For the differential rotation, we use the approximation by Belvedere, Kuzanyan & Sokoloff (2000) for helioseismological data

$$f(x,\theta) = \frac{1}{461}\sum_{m=0}^{2}\cos\left(2m\left(\frac{\pi}{2}-\theta\right)\right)\sum_{n=0}^{4}C_{nm}x^n. \quad (16)$$

The coefficients C_{mn} of this equation are given in Table 1 of Belvedere et al. (2000). Figure 1 shows the angular velocity isolines.

The kernel function of the nonlocal alpha-effect in the poloidal field equation (12) was prescribed as follows

$$\hat{\alpha}(x,x') = \frac{\phi_{\rm b}(x')\phi_\alpha(x)}{1+B^2(x',\theta)},$$
$$\phi_{\rm b}(x') = \frac{1}{2}\left(1-{\rm erf}\left((x'-x_{\rm b})/h_{\rm b}\right)\right),$$
$$\phi_\alpha(x) = \frac{1}{2}\left(1+{\rm erf}\left((x-x_\alpha)/h_\alpha\right)\right), \quad (17)$$

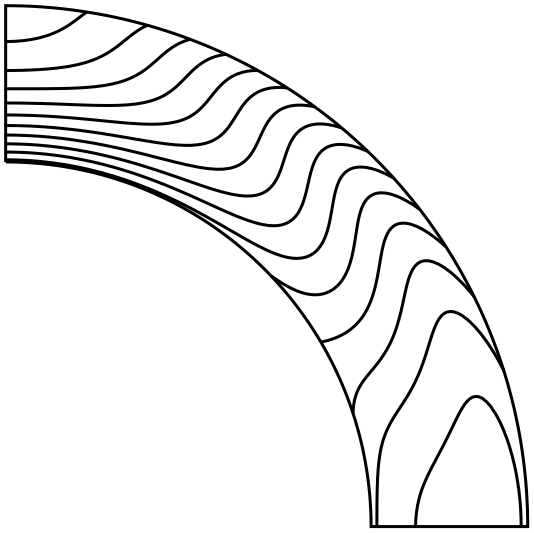

Fig. 1 Angular velocity isolines for the differential rotation used in the dynamo model.

where erf is the error function and B^2 in the denominator of the first equation accounts for the usual algebraic quenching of the alpha-effect. We always use $x_{\rm b} = x_{\rm i} + 2.5h_{\rm b}$ and $x_\alpha = 1 - 2.5h_\alpha$ to ensure smoothness of the kernel functions in the simulation domain. The $h_{\rm b}$-parameter is the thickness of the near-bottom region of toroidal magnetic fields producing the alpha-effect. The h_α is the thickness of the near-surface region where this alpha-effect is produced. The nonlocal alpha-effect with the kernel function (17) is very similar to the Babcock-Leighton mechanism for the poloidal field production used in the dynamo models of Durney (1995) and Dikpati & Charbonneau (1999).

To compare the results of the simulations for nonlocal and local alpha-effects we will need a local formulation of this effect, which can be obtained by applying the kernel function

$$\hat{\alpha}(x,x') = \frac{2\hat{\eta}\delta(x-x')}{1+B^2}. \quad (18)$$

The diffusivity profile of our model reads

$$\eta(x) = {\rm R_m^{-1}} + \frac{1}{2}(1-{\rm R_m^{-1}})\left(1+{\rm erf}\left(\frac{x-x_\eta}{h_\eta}\right)\right). \quad (19)$$

The aim of this paper is to demonstrate that the nonlocal alpha-effect is not prone to catastrophic quenching. We will do this with the following parameter values: $x_{\rm i} = 0.7$, $x_\eta = 0.74$, $h_\eta = 0.01$, $h_\alpha = 0.02$, $h_{\rm b} = 0.002$, and $R_\odot/\ell = 10$. The dependence on the model parameters will be discussed in a separate publication. The profiles of diffusivity and kernel functions (17) for this parameters set are shown in Fig. 2. The maximum value of the magnetic Reynolds number we were able to apply is ${\rm R_m} = 10^4$, and all the results of this paper were obtained with this value.

The system of dynamo equations (9), (12) and (13) was solved numerically with the grid-point method and explicit time-stepping. The diamagnetic pumping and low diffusion in the near-bottom region leads to a high concentration of

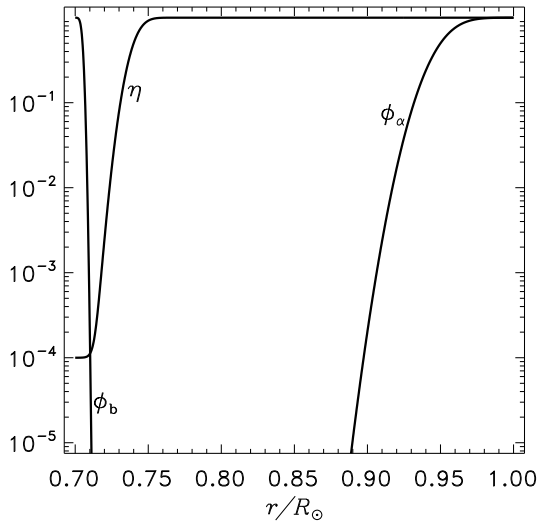

Fig. 2 Profiles of the normalised total diffusivity and the kernel functions (17) of the nonlocal alpha-effect.

the magnetic field near the bottom. To resolve the fine near-bottom structure, a nonuniform grid over the radius with the grid spacing $\Delta x \sim \eta^{1/2}$ was applied. The grid over the latitude was uniform. All the results of the next Section do not depend on numerical resolution. This was checked by repeating the runs with doubled resolution.

Equatorial symmetry was usually not prescribed. The field was evolved in time starting from a mixed-parity initial field and the solution relaxed eventually to a certain equatorial symmetry. In order to determine the critical dynamo numbers for excitation of the dipolar ($B(\theta) = -B(\pi - \theta)$) and quadrupolar ($B(\theta) = B(\pi - \theta)$) dynamo modes, additional boundary conditions selecting the field mode of certain equatorial symmetry were imposed on the equator.

3 Results and discussion

Our computations show that catastrophic quenching is present for local formulations of the alpha-effect but it does not exist for the model with a nonlocal alpha effect.

Figure 3 shows the results of computations for the local alpha-effect of Eq. (18). The upper line in this Figure was obtained with the $\alpha_{\rm M}$ put to zero in the poloidal field equation (12). Saturation of the dynamo in this case is due to the usual algebraic quenching of the alpha-effect. The lower line represents the computation with allowance for the magnetic alpha, $\alpha_{\rm M}$, governed by the dynamical equation (13). Magnetic energy considerably decreases in this case indicating catastrophic quenching of the dynamo.

In the model with the nonlocal alpha-effect of Eq. (17), saturation of the dynamo is due to the standard algebraic quenching only. The results of Fig. 4 for $\alpha_{\rm M}$ neglected or included are practically the same. When algebraic quenching is switched off by omitting B^2 in the denominator of the first equation of (17), but $\alpha_{\rm M}$ is kept finite, field growth

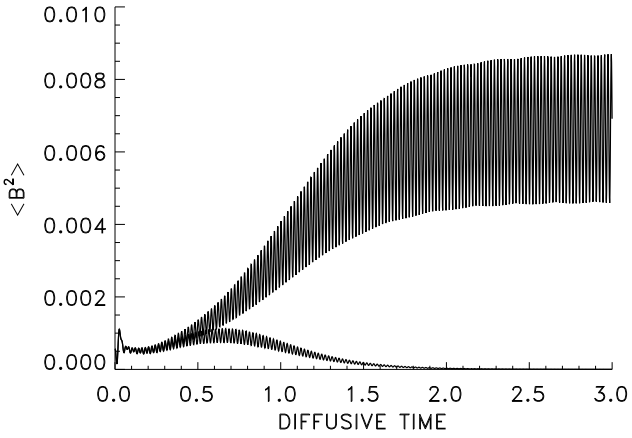

Fig. 3 Time dependencies of the volume-averaged square of the toroidal field $\langle B^2 \rangle$ for the runs with algebraic ($\alpha_{\rm M} = 0$, upper line) and catastrophic ($\alpha_{\rm M} \neq 0$) quenching of the local alpha effect of Eq. (18). Time is measured in units of $R_\odot^2/\eta_0$. The computations were performed for dynamo number $D = 5.3 \times 10^4$ slightly above the critical value of $D_{\rm c} = 5.0 \times 10^4$.

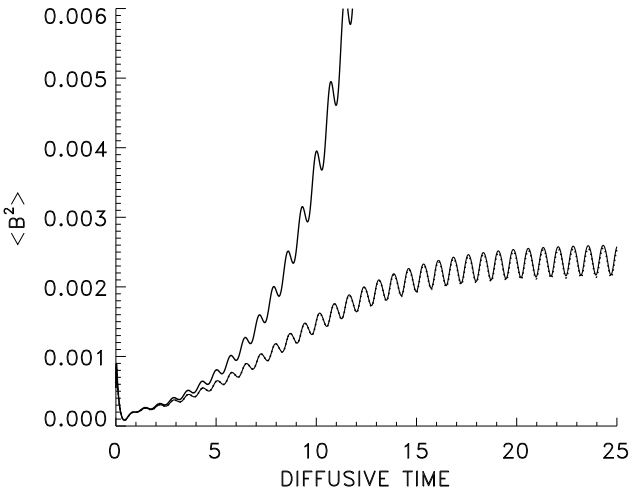

Fig. 4 Time dependencies of the mean square of the toroidal field in the model with nonlocal alpha-effect. The two bottom lines show the results of the runs with $\alpha_{\rm M} = 0$ (full line) and for the complete model ($\alpha_{\rm M} \neq 0$, dotted line). These two lines are hard to distinguish by eye. The upper line is for the computation neglecting the algebraic alpha-quenching. The field growth does not saturate in this case in spite of the finite $\alpha_{\rm M}$. The dynamo number $D = 2.2 \times 10^4$ is slightly above the critical value of $D_{\rm c} = 1.9 \times 10^4$.

does not saturate. Clearly, the $\alpha_{\rm M}$ does not play any role in these simulations.

The reason for the inefficiency of $\alpha_{\rm M}$ in the nonlocal dynamo model can be seen from Fig. 5, which shows the magnetic field patterns for several instances of a magnetic cycle. The toroidal field is highly concentrated at the bottom. It is small in the near-top region where the alpha-effect is active. In this case, the alpha-effect does not contribute to

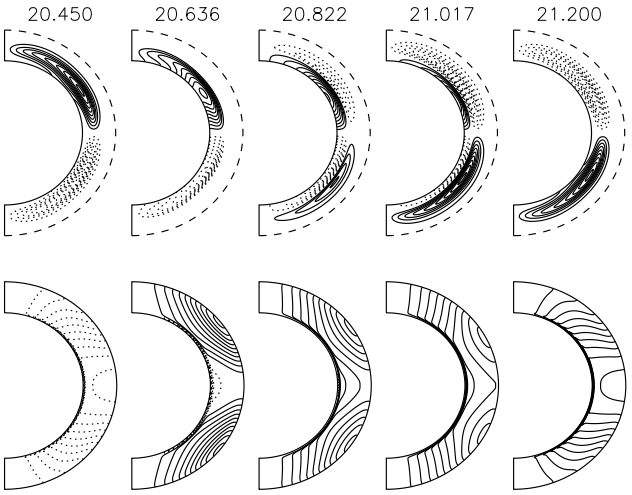

Fig. 5 Toroidal field isolines (top row) and poloidal filed lines (bottom row) for several instances of a magnetic cycle. The time of the run in units of $R_\odot^2/\eta_0$ is shown at the top. Full (dotted) lines show positive (negative) levels and clockwise (anticlockwise) circulation. The pictures of the upper row are rescaled so that the upper (dashed) boundary shows the radius of $r = 0.74R_\odot$ below which the toroidal fields are localized. $D = 2.2 \times 10^4$.

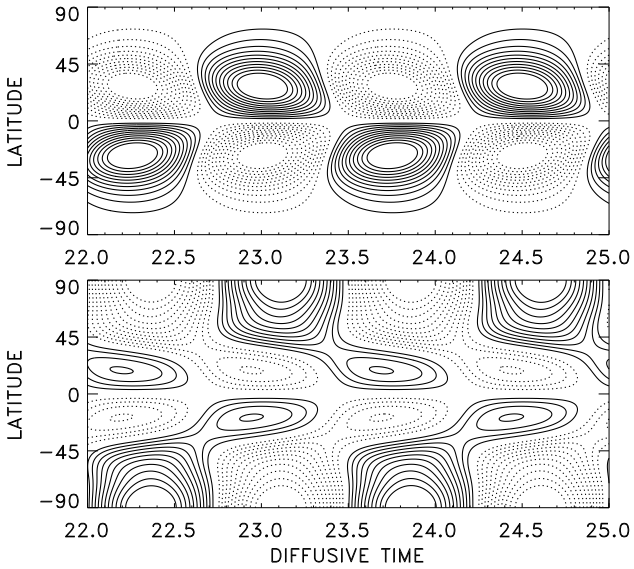

Fig. 6 Butterfly diagram of the depth-integrated toroidal field $\mathcal{B}$ of Eq. (20) (top panel) and surface radial field (bottom) for the model with nonlocal alpha-effect. Time is shown in units of $R_\odot^2/\eta_0$. $D = 2.2 \times 10^4$.

the first term on the right of the equation (3) and the generated large-scale fields are not helical. The small-scale magnetic helicity balancing the helicity of large-scale fields is not produced and the $\alpha_{\rm M}$ is small.

It should be noted that the non-locality of the alpha-effect alone does not guaranty nonoccurrence of catastrophic quenching. If the toroidal field in the near-top region of the alpha-effect has same sign and same order of magnitude as the near-bottom toroidal field that produces this alpha-effect, then catastrophic quenching can still happen (Brandenburg & Käpylä 2007). It can be imagined, however, that if such a distributed toroidal field has opposite signs near the top and near the bottom, then catastrophic *amplification* of the magnetic field will happen.

What excludes the catastrophic quenching in our model is the joint effect of non-locality and diamagnetic confinement of the toroidal field in the near-bottom region. This region has been long recognised as a favorable site for the solar dynamo (cf., e.g., Gilman 1992). The reason why the magnetic field should be concentrated at this site was not clear, however. We suggest that the concentration can be accounted for by diamagnetic pumping.

The poloidal field in Fig. 5 is also concentrated at the bottom. The following consideration shows that somewhere inside the sun the poloidal field must be much stronger than on the surface. The magnitude of the surface poloidal field is about 1-2 Gauss only. If the toroidal field is estimated by its magnitude in sunspots, it is about 1000 times stronger than the surface poloidal field. The solar differential rotation of about 30% can produce in the 11 years of the solar cycle a toroidal field that is at most 40 times stronger than the poloidal filed (the strong radial shear in the tachocline does not change this estimation because the radial field should be as much weaker there compared to the meridional field as the radial shear is larger than the latitudinal shear). Therefore, a poloidal field of several tens Gauss is necessary for the production of kilogauss toroidal fields. The toroidal field in our dynamo model is about 1000 times stronger than the polar field due to the near-bottom concentration of the poloidal field.

Figure 6 shows butterfly diagrams for the surface radial and deep toroidal fields. The toroidal field diagram shows the isolines of the quantity

$$\mathcal{B} = \sin\theta \int_{x_{\rm i}}^{1} \phi_{\rm b}(x) B(x)\, {\rm d}x, \qquad (20)$$

to which the Babcock-Leighton surface alpha-effect is proportional. The factor $\sin\theta$ in Eq. (20) accounts for the dependence of the length of toroidal flux tubes on latitude (it is supposed that the probability of sunspot production is proportional to the length of the tube).

The period of the magnetic cycles of Figures 4 and 6 equals $0.75R_\odot^2/\eta_0$, that for the diffusivity of $\eta_0 \approx 10^{13}\,{\rm cm}^2/{\rm s}$ is close to the 11 year period of the solar cycle. The model with nonlocal alpha-effect does not suffer from the old problem of too short magnetic cycles typical of the local dynamo models (Fig. 3).

The radial field diagram of Fig. 6 is similar to observational diagrams of Stenflo (1988) and Obridko et al. (2006).

The field pattern of Fig. 6 is antisymmetric about the equator. The critical dynamo number for excitation of the dipolar modes, $D_{\rm c}^{\rm d} = 1.9 \times 10^4$, is substantially smaller

than the critical number $D_{\rm c}^{\rm q} = 2.5 \times 10^4$ for the quadrupolar modes. Accordingly, the runs started from an initial field of mixed parity rapidly relaxed to dipolar parity. So clear preference for the dipolar modes is typical of the dynamo models with relative small magnetic diffusion near the base of the convection zone (Chatterjee, Nandy & Choudhuri 2004).

The only clear disagreement of the model with observations is the presence of toroidal fields in Fig. 6 on too high latitudes. It may be expected that even a slow meridional flow in the near-bottom region of low diffusion can influence the latitudinal profile of a toroidal field. Allowance for the meridional flow is a perspective for model improvement.

Acknowledgements. This work was supported by the Russian Foundation for Basic Research (projects 10-02-00148, 10-02-00391).

References

Belvedere, G., Kuzanyan, K.M., Sokoloff, D.D.: 2000, MNRAS 315, 778
Blackman, E., Brandenburg, A.: 2002, ApJ 579, 359
Brandenburg, A.: 2009, IAUS 259, 159
Brandenburg, A., Käpylä, P.J.: 2007, New J. Phys. 9, 305
Brandenburg, A., Subramanian, K.: 2005, Phys. Rep. 417, 1
Brandenburg, A., Jennings, R.L., Nordlund, Å., Rieutord, M., Stein, R.F., Tuominen, I.: 1996, JFM 306, 325
Chatterjee, P., Nandy, D., Choudhuri, A.R.: 2004, A&A 427, 1019
Dikpati, M., Charbonneau, P.: 1999, ApJ 518, 508
Dorch, S.B.F., Nordlund, Å.: 2001, A&A 365, 562
Durney, B.R.: 1995, Sol. Phys. 160, 213
Frisch, U., Pouquet, A., Léorat, J., Mazure, A.: 1975, J. Fluid Mech. 68, 769
Gilman, P.A.: 1992, in: K.L. Harvey (ed.), *The Solar Cycle*, ASP Conf. Series 27, 241
Gruzinov, A.V., Diamond, P.H.: 1994, Phys. Rev. Lett. 72, 1651
Guerrero, G., de Gouveia Dal Pino, E.M.: 2008, A&A 485, 267
Guerrero, G., Chatterjee, P., Brandenburg, A.: 2010, MNRAS 409, 1619
Kitchatinov, L.L., Rüdiger, G.: 2008, AN 329, 372
Kleeorin, N.I., Ruzmaikin, A.A.: 1982, Magnetohydrodyn. 18, 116
Kliem, B., Rust, S., Seehafer, N.: 2010, arXiv:astro-ph/1012.2297
Moffatt, H.K.: 1972, J. Fluid Mech. 53, 385
Obridko, V.N., Sokoloff, D.D., Kuzanyan, K.M., Shelting, B.D., Zakharov, V.G.: 2006, MNRAS 365, 827
Parker, E.N.: 1955, ApJ 122, 293
Rädler, K.-H.: 1968, Z. Naturforsch. 23a, 1851
Roberts, P.H., Soward, A.M.: 1975, AN 296, 49
Rüdiger, G.: 1974, AN 295, 275
Rüdiger, G., Brandenburg, A.: 1995, A&A 296, 557
Rüdiger, G., Kitchatinov, L.L.: 1993, A&A 269, 581
Spence, E.J., Nornberg, M.D., Jacobson, C.M., Parada, C.A., Taylor, N.Z., Kendrick, R.D., Forest, C.B.: 2007, PhRvL 98, 164503
Steenbeck, M., Krause, F., Rädler, K.-H.: 1966, Z.Naturforsch. 21a, 369
Stenflo, J.O.: 1988, Astrophys. Space Sci. 144, 321
Vainshtein, S.I., Cattaneo, F.: 1992, ApJ 393, 165
Vishniac, E.T., Cho, J.: 2001, ApJ 550, 752
Zeldovich, Ya.B.: 1957, JETP 4, 460
Ziegler, U., Rüdiger, G.: 2003, A&A 401, 433

